ELSEVIER

Journal of Alloys and Compounds 451 (2008) 297–300

Journal of ALLOYS AND COMPOUNDS

www.elsevier.com/locate/jallcom

# Microwave-assisted synthesis and characterization of ultrafine neodymium oxide particles

Mirosław Zawadzki *

*Institute of Low Temperature and Structure Research, Polish Academy of Sciences, PO Box 1410 Wrocław 2, Poland*

Available online 13 April 2007

**Abstract**

Nanocrystalline neodymium oxide precursor particles have been prepared for the first time by a microwave-assisted hydrothermal route from a solution containing $Nd(CH_3COO)_3 \cdot H_2O$. Further thermal treatment of the as-prepared precursors resulted in the formation of the well-crystallized $Nd_2O_3$ (cubic or trigonal) nanoparticles with fibrous or rod-like morphology. It was found that neodymium oxide is mesoporous material owning the specific surface area up to 130 $m^2/g$. The proposed synthesis, in contrast to conventional hydrothermal method, offers very rapid heating with better yield and high reproducibility.


*Keywords:* Microwave-assisted hydrothermal synthesis; Neodymium oxide; Nanoparticles

## 1. Introduction

Hydrothermal methods, which involve low temperatures and wet chemical technique, offer the possibility for the synthesis of high-purity, homogeneous, and ultrafine materials. In particular, the use of microwaves as the heating source may offer benefits in terms of cost savings through the reduction in processing time and energy input and may result in improved product yields [1]. Due to the properties of internal and volumetric heating, thermal gradients during microwave processing are avoided, providing a uniform environmental for reaction and the consequent dramatic increase in reaction rates. Recently, the application of microwave irradiation to materials science has shown rapid growth due to its usefulness in the preparation of a variety of nanosized inorganic materials [2,3]. Compared with conventional heating, microwave heating has an advantage of high-efficiency and rapid formation of nanoparticles with a narrow size distribution and no serious agglomeration. In particular, microwave-assisted hydrothermal (or more generally solvothermal) method may be very useful in production of finely dispersed, nanocrystalline materials of great technological importance [4,5]. To such group of materials belong nanocrystalline rare earth oxides. Among them, neodymium oxide has been attracting a great deal of interest due to its unique properties and applications in various fields as luminescent materials [6], catalysts [7], protective coatings or components for advanced ceramic materials [8].

Rare earth oxides are usually produced by oxalic acid precipitation in industry. By that procedure, the products are pure and easily filtered but the size of the powders is in the range of micrometers [9]. In order to get ultrafine rare earth oxide particles, such routs as chemical vapor deposition, laser ablation, sol–gel processes, polyol method, *etc*. can be used. At the nanometer scale $Nd_2O_3$ is reported to have been elaborated only in the form of agglomerated powders by microemulsion technique [10], sol gel auto-combustion [11], hydrogen plasma-metal reaction [12]. Recently, hydrothermal methods have been successfully applied for the preparation of dispersed neodymium oxide nanoparticles with various morphology [13]. In this paper the preparation of nanocrystalline neodymium oxide precursors for the first time by a microwave-assisted hydrothermal route is reported.

## 2. Experimental

### 2.1. Samples

Neodymium acetate hydrate, prepared in our laboratory, was used as starting material. XRD pattern of the acetate (not shown) corresponded well with the pattern calculated from the single crystal data of $Nd(ac)_3 \cdot H_2O$ as reported by Junk et al. [14]. Other reagents were of analytical grade and used without further purification. Neodymium acetate was prepared by slow dissolution of the oxide (Aldrich) in a hot acetic acid (glacial) followed by a vacuum evaporation of

* Tel.: +48 71 3435021; fax: +48 71 3441029.
*E-mail address:* m.zawadzki@int.pan.wroc.pl.

0925-8388/$ – see front matter © 2007 Elsevier B.V. All rights reserved.
doi:10.1016/j.jallcom.2007.04.060

the excess acid at room temperature. 1.96 g acetate was added to 50 ml distilled water (previously degassed at boiling temperature in order to remove $CO_2$) with continuous stirring until it was completely dissolved. The microwave-assisted hydrothermal synthesis were performed in a microwave accelerated reaction system MW Reactor ERTEC Model 02-02, described elsewhere [15], which operates at 2.45 GHz frequency with 0–100% of full power (1000 W). A microwave accelerated reaction system equipped with a teflon vessel of 70 ml capacity was filled with the prepared solution up to 70% of the total volume. The reactor was sealed and then the vessel was microwave heated to the desired temperature (220 and 290 °C, respectively, for samples A and B) at a rate of 15 °C/min. The pressure of the reactor gradually increased, about 20 and 40 bar, respectively, and maintained during the holding period (1 and 4 h, respectively, for samples A and B). The light violet product was obtained which was washed at least five times by repeated cycles of centrifugation and re-dispersion in deionized water. Finally, the nanoparticles in the product were concentrated and separated from the solvent by centrifugation and subsequent vacuum drying at room temperature for several hours. Conventional thermal treatment of the as-prepared powder was performed at temperatures up to 800 °C for 4 h to obtain the well-crystallized neodymium oxide.

### 2.2. Methods of characterization

The structure and crystallinity of the samples were characterized by X-ray powder diffraction (XRD) method. The XRD data were collected using DRON-3 diffractometer with Cu Kα radiation. The ICDD database was utilized for phase identification. The average crystallite size $D$ of $Nd_2O_3$ was calculated using the Schererr equation [16] from the broadening of the X-ray line (2 2 2) and (1 0 1), for C and A type oxide, respectively, which was calibrated from high purity silicon.

Transmission electron micrographs (TEM) and corresponding electron diffraction patterns (SAED) of the samples were obtained by using Tesla BS 500 microscope at 90 kV. Samples for the TEM observations were prepared by ultrasonically dispersing the powders in water and putting a droplet of the suspension on a copper microscope grid covered with perforated carbon.

The textural properties of samples (specific surface area and porosity) were determined by nitrogen adsorption–desorption isotherms at liquid nitrogen temperature by using an automatic volumetric apparatus (FISONS Sorptomatic 1900). Prior to measuring, all samples were degassed at 250 °C for some hours and $10^{-3}$ Torr. Specific surface areas, $S_{BET}$, were measured by the Brunauer–Emmett–Teller (BET) method. The pore distribution was analyzed following the Dollimore–Heal (D–H) method, which was applied to the desorption branch of each isotherm.

## 3. Results and discussion

Phase composition and morphology of the samples prepared under microwave-assisted hydrothermal conditions from $Nd(ac)_3 \cdot H_2O$ precursor depend on the reaction parameters.

Fig. 1 shows XRD patterns of product A (220 °C, 1 h), as-prepared and heated at various temperatures. The analysis of the pattern for the as-prepared sample (Fig. 1a) indicates that it could not be assigned to any known neodymium compound [17]. It resembles to some extent the pattern of neodymium hydroxide but the presence of a strong reflection at low $2\theta$ angle suggest that the structure may be similar to that observed in layered hydrox-

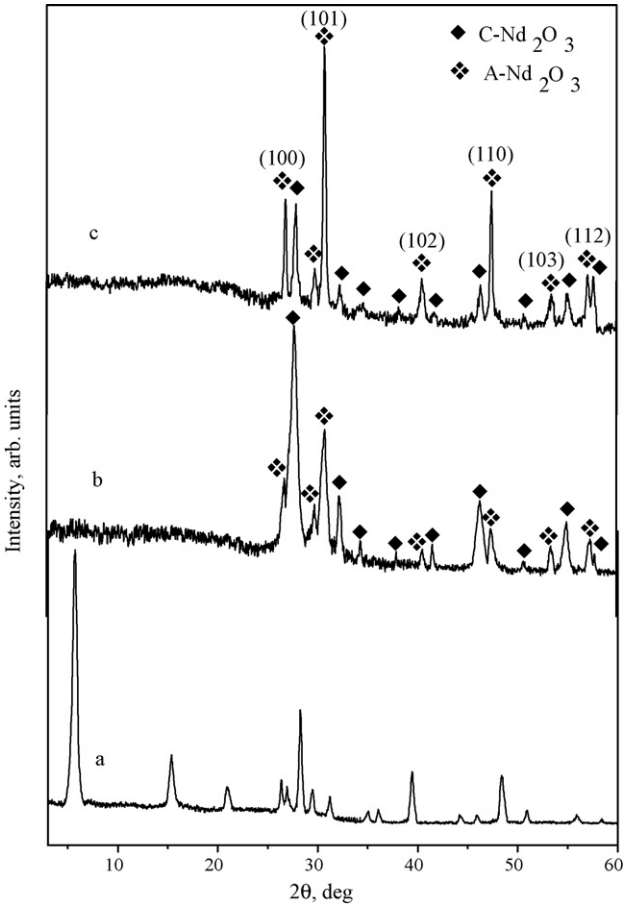


Fig. 1. XRD patterns of product A: (a) as-prepared; (b) heated at 600 °C; (c) heated at 800 °C.

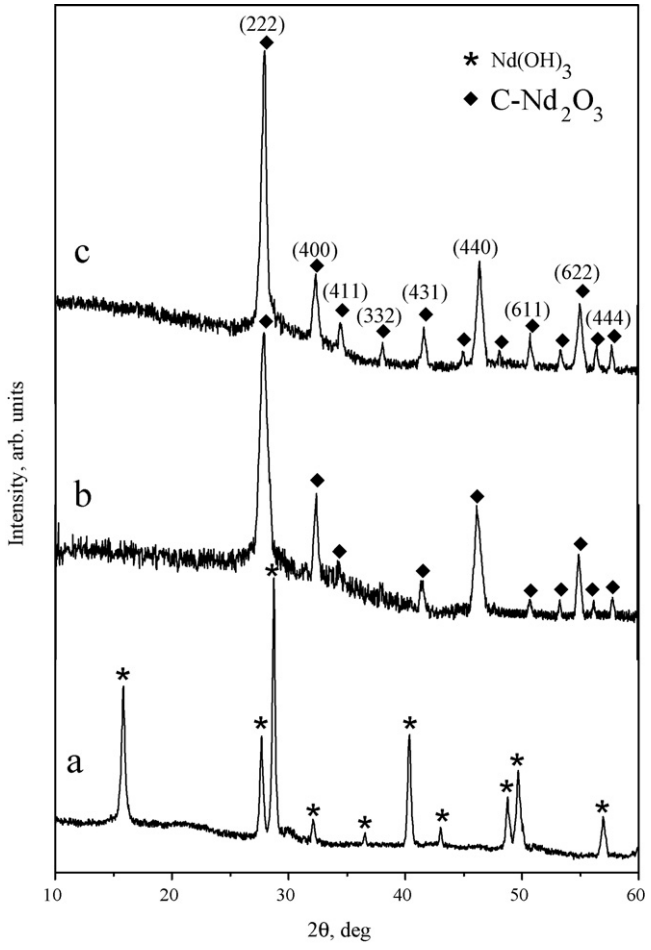


Fig. 2. XRD patterns of product B: (a) as-prepared; (b) heated at 600 °C; (c) heated at 800 °C.

ide metal acetates [18]. After heat treatment the strongest low angle reflection disappears and complete reordering of the sample with crystallization of neodymium oxide phase was noticed. In particular, when product A is heated at 600 °C (Fig. 1b) crystalline reflections appear in the pattern, which could be assigned, to two forms of $Nd_2O_3$: cubic [19] and trigonal [20], respectively as major and minor phase. Further treatment at 800 °C (Fig. 1c) leads to crystallization of trigonal phase (A-$Nd_2O_3$) but some amounts of cubic phase (C-$Nd_2O_3$) is still detected. The average crystallite size of neodymium oxide particles, calculated from the half-width of the diffraction peaks, increases from about 9 nm (cubic phase) to 17 nm (trigonal phase) as the heating temperature rises from 600 to 800 °C.

The XRD results of the product B (290 °C, 4 h) thermal evolution are presented in Fig. 2. It is seen that the as-prepared sample (Fig. 2a) matched well with the pattern of $Nd(OH)_3$ calculated from single crystal data [21]. After further heat treatment the hydroxide transformed completely into cubic oxide. The phase identification reveals the characteristic patterns of C-$Nd_2O_3$ and no other phases are detected after heating up to 800 °C. According to literature cubic neodymium oxide is observed during decomposition of $Nd(OH)_3$ at temperature range from

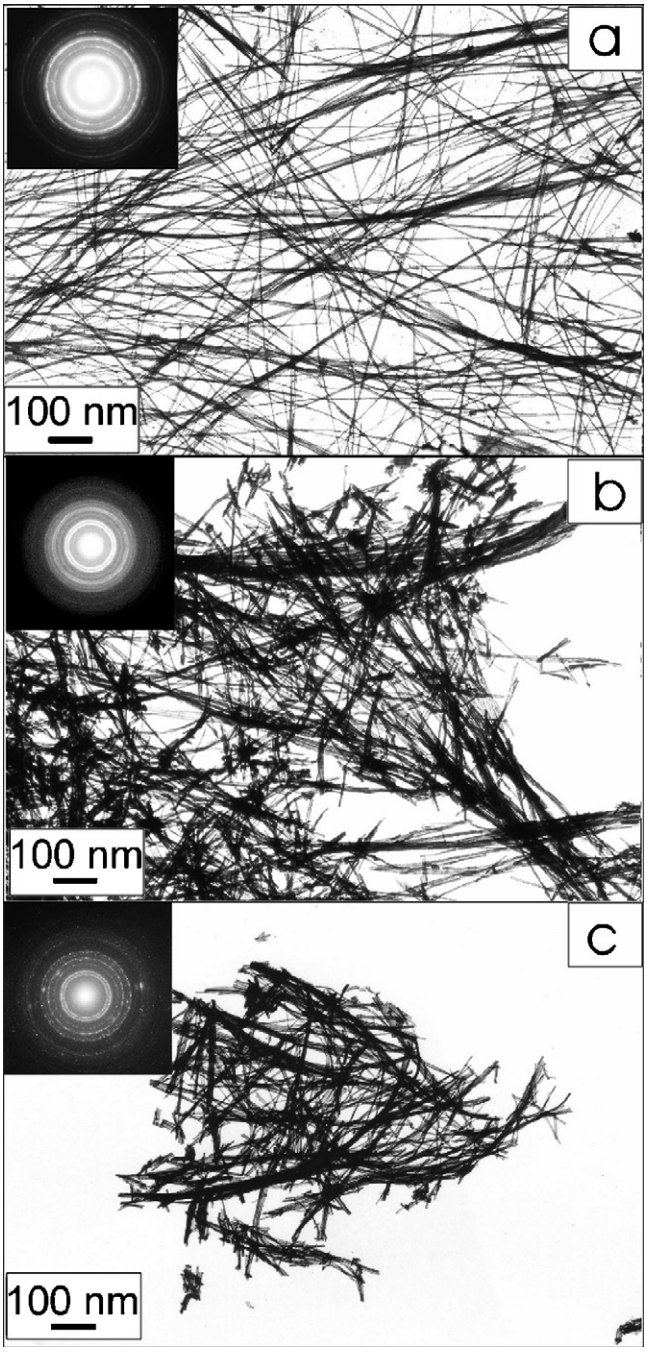


Fig. 3. TEM micrographs of product A: (a) as-prepared; (b) heated at 600 °C; (c) heated at 800 °C; with corresponding SAED patterns.

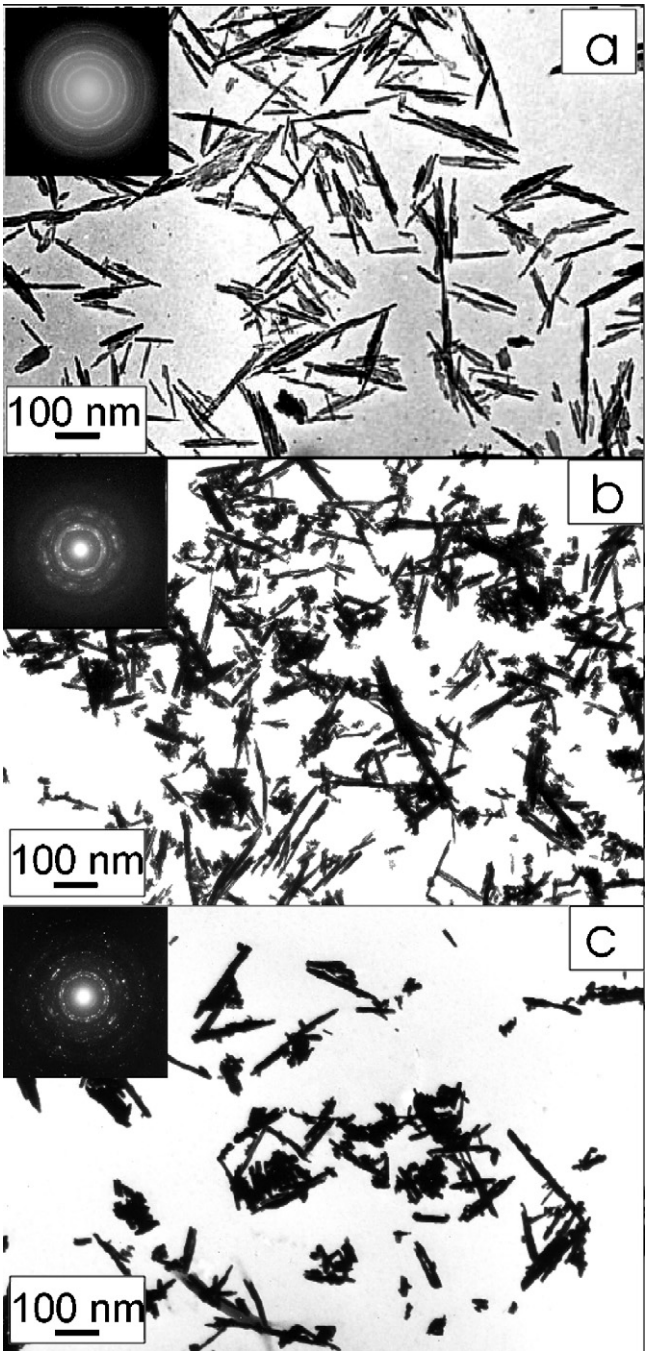


Fig. 4. TEM micrographs of product B: (a) as-prepared; (b) heated at 600 °C; (c) heated at 800 °C; with corresponding SAED patterns.

400 to 600 °C, and then progressive transformation into trigonal phase occurs [22]. Our results indicate that neodymium hydroxide obtained by microwave-assisted hydrothermal method (at severe conditions) is suitable precursor when preparing $Nd_2O_3$ with preserved cubic structure is necessary. It should be also noticed that the average crystallite size of C-$Nd_2O_3$ particles was changed slightly from 10 to 14 nm when heating temperature was raised from 600 to 800 °C. It also suggests good thermal stability of neodymium oxide obtained from sample B as precursor.

Fig. 3 shows microstucture and morphology evolution of the product A after heat treatment up to 800 °C. From TEM image (Fig. 3a) for the as-prepared sample, the arrays of fibrous nanoparticles randomly oriented are observed with the particle size of the length in micrometer range and the thickness from 6 nm, and some of them are slightly aggregated into bundles due to the higher surface energy of the nanoparticles. SAED pattern from the sample contains broad rings typical for amorphous materials. After heat treatment (Fig. 3b and c) the fibers preserve their shape, though become shorter and often stick together to form belts up to tens nanometers. In SAED patterns well-developed rings of cubic and trigonal $Nd_2O_3$ are seen, respectively, for the sample heated at 600 and 800 °C.

TEM micrographs of the product B, as-prepared and after further heating are shown in Fig. 4. SAED and TEM revealed that the as-prepared sample (Fig. 4a) consists of $Nd(OH)_3$ rod-like crystals with diameter from 7 nm and length up to 300 nm. When sample B is heated at 600 °C (Fig. 4b) or even at 800 °C (Fig. 4c), the shape of the particles is preserved however some signs of aggregation occur and an increase in the particle diameter is also noticeable. Both SAED patterns (at 600 and 800 °C) exhibit C-$Nd_2O_3$ structure of particles.

Textural analysis was performed on the sample A and B after thermal treatment at 600 °C which results in the formation of $Nd_2O_3$. Fig. 5 compares the nitrogen adsorption–desorption isotherms and corresponding pore size distribution for studied samples. The both samples show type IV isotherms with a H1 and H2 hysteresis loop, respectively for samples A and B (according to IUPAC classification [23]). This means, that $Nd_2O_3$ is mesoporous material with a very low contribution of micropores, responsible for the adsorption observed at low pressure $P/P_0 < 0.1$. Inset on Fig. 5 indicates that both samples have broad monomodal pore size distribution, centered at 4.3 and 6.1 nm for the samples A and B, respectively. It should be noticed, however, that the most of pore diameters include in the range of 2–10 nm. It was found that specific surface area is 130 and 90 $m^2/g$ for the samples A and B, respectively.

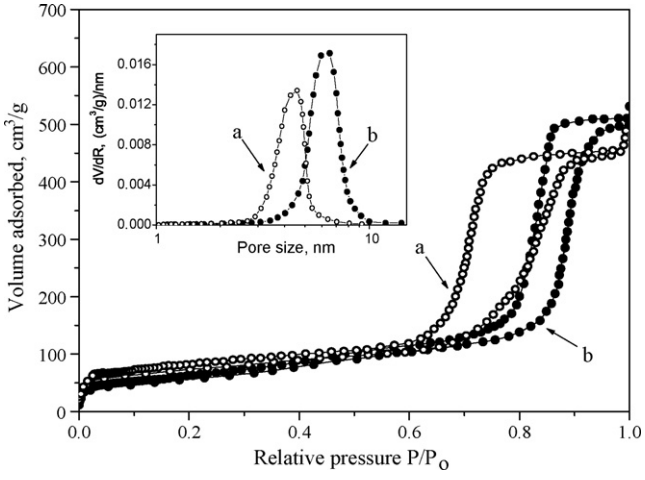


Fig. 5. Nitrogen adsorption–desorption isotherms and pore size distribution of product A (a) and product B (b) heated at 600 °C.

## 4. Conclusions

The nanocrystalline neodymium oxide precursors of different morphology were successfully obtained under hydrothermal conditions using microwave heating for a relatively short time. It was found that the reaction parameters such as temperature/pressure and hold time determined morphology, as well as crystal structure. At mild conditions very long fibrous nanoparticles are formed while shorter rod-like particles are obtained at serve conditions (higher temperature/pressure and prolonged time). After heating both products reveals $Nd_2O_3$ structure (cubic or trigonal) with interesting textural properties including high surface area, mesoporosity with pore size distribution below 10 nm.

## References

[1] S. Komarneni, Curr. Sci. 85 (12) (2003) 1730.
[2] W.X. Tu, H.F. Liu, Chem. Mater. 12 (2000) 564.
[3] M. Shen, Y.K. Du, N.P. Hua, P. Yang, Powder Technol. 161 (1) (2006) 64.
[4] S. Baldassari, S. Komarneni, E. Mariani, C. Villa, Mater. Res. Bull. 40 (11) (2005) 2014.
[5] V.S.R. Raju, S.R. Murthy, F. Gao, Q. Lu, S. Komareni, J. Mater. Sci. 41 (5) (2006) 1475.
[6] R. Bazzi, A. Brenier, P. Perriat, O. Tillement, J. Lumin. 113 (2005) 161.
[7] K. Byrappa, M.H. Sunitha, A.K. Subramani, S. Ananda, K.M. Lokanatha Rai, B. Basavalingu, M. Yoshimura, J. Mater. Sci. 41 (2006) 1369.
[8] S. Chevalier, G. Bonnet, J.P. Laprin, Appl. Surf. Sci. 167 (2000) 125.
[9] J.Y. Wu, W. Gao, F. Zhang, Chinese Rare-earths 2 (2001) 5.
[10] Q. Wenxiu, S. Buddhudu, Y. Zhou, Y.L. Lam, J. Zhou, Y.C. Chan, C.H. Kam, L.H. Gan, G. Roshan Deen, Mater. Sci. Eng. C 16 (2001) 153.
[11] W. Yang, Y. Qi, Y. Ma, X. Li, X. Guo, J. Gao, M. Chen, Mater. Chem. Phys. 84 (2004) 52.
[12] T. liu, Y.H. Zhang, H.Y. Shao, X.G. Li, Langmuir 19 (18) (2003) 7569.
[13] L. Kepinski, M. Zawadzki, W. Mista, Solid State Sci. 6 (2004) 1327.
[14] P.C. Junk, C.J. Kepert, L. Wei-Min, B.W. Skelton, A.H. White, Aust. J. Chem. 52 (1999) 437.
[15] M. Zawadzki, Solid State Sci. 8 (2006) 14.
[16] H.P. Klug, L.E. Alexander, X-ray Diffraction Procedure for Polycrystalline and Amorphous Material, Wiley, New York, 1974.
[17] International Centre for Difraction Date, ICDD, PDF-4+2005.
[18] L. Poul, N. Jouini, F. Fievet, Chem. Mater. 12 (2000) 3123.
[19] ICDD PDF No. 21-0579.
[20] ICDD PDF No. 41-1089.
[21] G.W. Beall, W.O. Milligan, D. Dillin, R. Williams, J. McCoy, Acta Crystallogr. B 32 (1976) 2227.
[22] P.P. Fedorov, M.V. Nazarkin, R.M. Zakalyukin, Crystallogr. Rep. 47 (2002) 281.
[23] International Union of Pure and Applied Chemistry, IUPC, Pure Appl. Chem. 57 (1985) 603.